Novel Classification Schemes for Radar Scenarios: Design and Comparison

Chaoran Yin
Institute of Acoustics, Chinese Academy of Sciences, 100190 Beijing, China, and University of Chinese Academy of Sciences, 100049 Beijing, China
E-mail: yinchaoran18@mails.ucas.ac.cn

Linjie Yan
Institute of Acoustics, Chinese Academy of Sciences, 100190 Beijing, China,
E-mail: yanlinjie16@163.com

Chengpeng Hao
Institute of Acoustics, Chinese Academy of Sciences, 100190 Beijing, China
E-mail: haochengp@mail.ioa.ac.cn

Silvia Liberata Ullo
Engineering Department,University of Sannio, 82100 Benevento, Italy
E-mail: ullo@unisannio.it

Danilo Orlando
Università degli Studi Niccolò Cusano, 00166 Rome, Italy
E-mail: danilor78@gmail.com

Chaohuan Hou
Institute of Acoustics, Chinese Academy of Sciences, 100190 Beijing, China
E-mail: hch@mail.ioa.ac.cn

***Abstract*—This paper addresses the classification of the operating scenario in radar applications in terms of data homogeneity. Specifically, we consider configurations accounting for homogeneous, partially-homogeneous, and clutter edge environments. This is an essential issue since such an information allows us to derive the most appropriate target detection schemes for the current scenario. To this end, we resort to a heuristic design procedure and come up with a classification architecture obtained by cascading two binary hypothesis tests that are solved by means of the generalized likelihood ratio test (GLRT) criterion. At the design stage, we first assume that the rank of the clutter covariance matrix is known and derive the GLRT, then we devise a preliminary stage for rank estimation when it is unknown. Illustrative examples show the effectiveness of both the preliminary stage and the classification architecture.**

I. Introduction

In the radar context, clutter classification is a relevant issue to accomplish an effective target detection through suitable decision rules obtained, for instance, by applying the generalized likelihood ratio test (GLRT). A preliminary analysis of the surrounding environment becomes a crucial objective in radar systems. The most common design assumption, namely the homogeneous environment where both the secondary and the primary data maintain the same clutter properties, is no longer sufficient to handle a real situation with interactions among all the backscattered signals due to the multiple propagation pathways. To reduce unwanted contributions with respect to the signal of interest containing the target, it is essential to tackle the clutter correctly and in order to do that, the clutter characterization is a cumbersome operation. For years the target detection problem has been carried out through the classical hypothesis of homogeneous environments, where the signal of interest was embedded in a Gaussian noise [1]–[6]. Yet, very quickly it has appeared clear that new insights were necessary and more articulated models have been designed to take into account partially-homogeneous environments [7]–[13], with the extension to the case where a Clutter edge is considered [14].

It is important to notice that, in both of the above mentioned non-homogeneous situations, the detection schemes devised under homogeneous assumption might experience significant performance degradations due to low covariance estimation quality, and can no longer guarantee the constant false alarm rate (CFAR) properties. On the other hand, when the power transitions are negligible, the homogeneous detectors have to be preferred for their effectiveness and low computational burden. Thus, it would be highly desirable to devise a classification architecture which is capable of identifying the real radar working scenarios. As a matter of fact, such *a priori* information allows to drive the systems toward the best choice of detection schemes whose performance is optimized under the current operating scenario [15]. One of the most known strategies dealing with the possible heterogeneity and clutter edges is the Variable Index CFAR algorithm [16], which is capable of identifying the background by comparing test statistics with thresholds. In [17], the strategy for clustering heterogeneous data into homogeneous subsets has been proposed exploiting the Expectation Maximization algorithm [18]. The most recent effort on the background classification in terms of homogeneity consists in detecting the clutter edge by means of GLRT criterion [14].

The *a priori* knowledge of the surrounding environment in a target-detection radar systems has also inspired the present work, where a novel classification scheme for radar scenarios is introduced and discussed. Specifically, we jointly consider the homogeneous, partially-homogeneous, and the clutter-edge-present cases. To this end, we come up with a heuristic architecture which is a cascade of two binary test stages solved by GLRT. The clutter edge scenario is rejected at the first stage by understanding the homogeneity of the secondary data, and at the second stage we classify between the homogeneous and partially-homogeneous environments resorting to the overall data set. At the design stage, we first assume that the rank

of the clutter covariance matrix is known, and then devise an estimation stage to deal with the case when it is unknown. Simulations results show the effectiveness of both the rank estimation stage and the proposed classification architecture.

The remainder of the paper is organized as follows. The next section contains the problem formulation and preliminary definitions, whereas Section III is devoted to the design of the classification architecture. Illustrative examples are provided in Section IV and we conclude the paper in Section V.

A. Notation

In the sequel, vectors (matrices) are denoted by boldface lower (upper) case letter. Superscripts $(\cdot)^T$ and $(\cdot)^\dagger$ denote transpose and complex conjugate transpose, respectively. We denote by $\boldsymbol{S}(i,j)$ the (i,j)-th element in the matrix $\boldsymbol{S}$. $\mathbb{R}^{m\times n}$ and $\mathbb{C}^{m\times n}$ are real and complex matrix spaces of dimension $m\times n$. $\boldsymbol{I}$ stands for an identity matrix of suitable dimension. $\mathcal{CN}_N(\boldsymbol{\mu},\boldsymbol{X})$ denotes the N-dimensional circular complex Gaussian distribution with mean $\boldsymbol{\mu}$ and covariance matrix $\boldsymbol{X}$. $\det(\cdot)$ represents the determinant of a matrix and the modulus of a scalar, and $\mathrm{Tr}(\cdot)$ denotes the trace of a square matrix. $\jmath=\sqrt{-1}$ and $U(0,1)$ the uniformly distributed random variable on the interval from 0 to 1.

II. Problem Formulation and Preliminary Definitions

Consider a radar system equipped with $N\geq 2$ space and/or time channels illuminating the surveillance area. We assume that the system performs the decision over a set of primary data [5], [19] denoted by $\boldsymbol{z}_k\in\mathbb{C}^{N\times 1}$, $k=1,\ldots,K_P$, corresponding to K_P consecutive cells under test (CUTs). Furthermore, we denote by $\boldsymbol{r}_k\in\mathbb{C}^{N\times 1}$, $k=1,\ldots,K_S$, a set of secondary data gathered from the leading and lagging window [20] in the proximity of the CUTs. At the design stage, all data are assumed IID circularly symmetric complex Gaussian random vectors with zero mean and positive definite covariance matrix.

Therefore, the classification problem for the radar scenarios can be formulated in terms of the following multiple hypothesis test

$$\begin{cases} H_0: \begin{cases} \boldsymbol{z}_k\sim\mathcal{CN}_N(\boldsymbol{0},\sigma^2\boldsymbol{I}+\boldsymbol{M}), & k=1,\ldots,K_P,\\ \boldsymbol{r}_k\sim\mathcal{CN}_N(\boldsymbol{0},\sigma^2\boldsymbol{I}+\boldsymbol{M}), & k=1,\ldots,K_S,\end{cases}\\ H_1: \begin{cases} \boldsymbol{z}_k\sim\mathcal{CN}_N(\boldsymbol{0},\sigma^2\boldsymbol{I}+\boldsymbol{M}), & k=1,\ldots,K_P,\\ \boldsymbol{r}_k\sim\mathcal{CN}_N(\boldsymbol{0},\sigma^2\boldsymbol{I}+\boldsymbol{M}_1), & k=1,\ldots,K_S,\end{cases}\\ H_2: \begin{cases} \boldsymbol{z}_k\sim\mathcal{CN}_N(\boldsymbol{0},\sigma^2\boldsymbol{I}+\boldsymbol{M}), & k=1,\ldots,K_P,\\ \boldsymbol{r}_k\sim\mathcal{CN}_N(\boldsymbol{0},\sigma^2\boldsymbol{I}+\boldsymbol{M}), & k=1,\ldots,K_1,\\ \boldsymbol{r}_k\sim\mathcal{CN}_N(\boldsymbol{0},\sigma^2\boldsymbol{I}+\boldsymbol{M}_2), & k=K_1+1,\ldots,K_S,\end{cases}\end{cases} \tag{1}$$

where $\sigma^2\boldsymbol{I}$ is the thermal noise component with $\sigma^2>0$ the unknown noise power level; $\boldsymbol{M}\in\mathbb{C}^{N\times N}$ is the clutter covariance matrix whose rank, $r<N$, is for the moment assumed known, $K_P>r$ and $K_S>r$; $\boldsymbol{M}_l\in\mathbb{C}^{N\times N}$, $l=1,2$ are defined as $\boldsymbol{M}_l=\boldsymbol{U}\boldsymbol{\Gamma}_l\boldsymbol{\Lambda}\boldsymbol{\Gamma}_l\boldsymbol{U}^\dagger$, $l=1,2$, where $\boldsymbol{\Lambda}=diag\,(\lambda_1,\ldots,\lambda_r,0,\ldots,0)$, $\lambda_1\geq\ldots\geq\lambda_r>0$, contains the eigenvalues of $\boldsymbol{M}$, $\boldsymbol{U}$ is the unitary matrix of the corresponding eigenvectors, $\boldsymbol{\Gamma}_l=diag(\sqrt{\gamma_{1,l}},\ldots,\sqrt{\gamma_{r,l}},0,\ldots,0)$, $\gamma_{1,l}\geq\ldots\geq\gamma_{r,l}>0$, $l=1,2$, represent possible power variations of the clutter along different directions. $K_1\in\{r,\ldots,K_S-r\}$ is the unknown positions of the clutter power transitions within the lagging or leading windows under H_2.

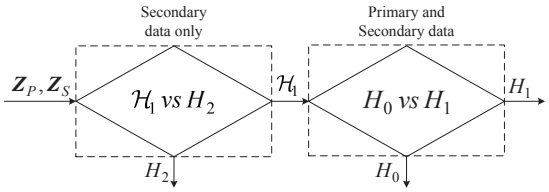

Fig. 1: Classification architecture diagram

In (1), H_0 is the homogeneous environment, where the clutter component in the primary and secondary data share the same statistical characterization, whereas H_1 is the well-known partially-homogeneous environment, where clutter in the primary and secondary data share the same clutter covariance structure up to a scaling factor [1], and H_2 is the non-homogeneous environment where secondary data contains a clutter edge coming from either the lagging or the leading window [14];

Let us denote by $\boldsymbol{Z}_P=[\boldsymbol{z}_1,\ldots,\boldsymbol{z}_{K_P}]\in\mathbb{C}^{N\times K_P}$, $\boldsymbol{Z}_S=[\boldsymbol{r}_1,\ldots,\boldsymbol{r}_{K_S}]\in\mathbb{C}^{N\times K_S}$, and $\boldsymbol{Z}=[\boldsymbol{Z}_P,\boldsymbol{Z}_S]\in\mathbb{C}^{N\times(K_P+K_S)}$ the overall data set. Based upon the above assumptions, the probability density function (PDF) of $\boldsymbol{Z}$ under H_i, $i=0,1,2$, namely $f_i(\boldsymbol{Z};\boldsymbol{\theta}_i)$ can be expressed as $f_i(\boldsymbol{Z};\boldsymbol{\theta}_i)=f_P(\boldsymbol{Z}_P;\sigma^2,\boldsymbol{M})f_{S_i}(\boldsymbol{Z}_S;\boldsymbol{\theta}_i)$, $i=0,1,2$, where

$$\begin{cases} f_P(\boldsymbol{Z}_P;\sigma^2,\boldsymbol{M})=\left[\frac{\exp\left\{-\frac{1}{K_P}\sum_{k=1}^{K_P}\boldsymbol{z}_k^\dagger(\sigma^2\boldsymbol{I}+\boldsymbol{M})^{-1}\boldsymbol{z}_k\right\}}{\pi^N\det(\sigma^2\boldsymbol{I}+\boldsymbol{M})}\right]^{K_P}\\ f_{S_0}(\boldsymbol{Z}_S;\boldsymbol{\theta}_0)=\left[\frac{\exp\left\{-\frac{1}{K_S}\sum_{k=1}^{K_S}\boldsymbol{r}_k^\dagger(\sigma^2\boldsymbol{I}+\boldsymbol{M})^{-1}\boldsymbol{r}_k\right\}}{\pi^N\det(\sigma^2\boldsymbol{I}+\boldsymbol{M})}\right]^{K_S}\\ f_{S_1}(\boldsymbol{Z}_S;\boldsymbol{\theta}_1)=\left[\frac{\exp\left\{-\frac{1}{K_S}\sum_{k=1}^{K_S}\boldsymbol{r}_k^\dagger(\sigma^2\boldsymbol{I}+\boldsymbol{M}_1)^{-1}\boldsymbol{r}_k\right\}}{\pi^N\det(\sigma^2\boldsymbol{I}+\boldsymbol{M}_1)}\right]^{K_S}\\ f_{S_2}(\boldsymbol{Z}_S;\boldsymbol{\theta}_2)=\left[\frac{\exp\left\{-\frac{1}{K_1}\sum_{k=1}^{K_1}\boldsymbol{r}_k^\dagger(\sigma^2\boldsymbol{I}+\boldsymbol{M})^{-1}\boldsymbol{r}_k\right\}}{\pi^N\det(\sigma^2\boldsymbol{I}+\boldsymbol{M})}\right]^{K_1}\times\\ \qquad\left[\frac{\exp\left\{-\frac{1}{K_C}\sum_{k=K_1+1}^{K_S}\boldsymbol{r}_k^\dagger(\sigma^2\boldsymbol{I}+\boldsymbol{M}_2)^{-1}\boldsymbol{r}_k\right\}}{\pi^N\det(\sigma^2\boldsymbol{I}+\boldsymbol{M}_2)}\right]^{K_C}\end{cases} \tag{2}$$

with $\boldsymbol{\theta}_0=\left[\sigma^2,\boldsymbol{\nu}^T(\boldsymbol{M})\right]^T$, $\boldsymbol{\theta}_1=\left[\boldsymbol{\theta}_0^T,\boldsymbol{\nu}^T(\boldsymbol{M}_1)\right]^T$, $\boldsymbol{\theta}_2=\left[\boldsymbol{\theta}_0^T,K_1,\boldsymbol{\nu}^T(\boldsymbol{M}_2)\right]^T$, $K_C=K_S-K_1$, and $\boldsymbol{\nu}(\boldsymbol{M})$ the vector-valued function selecting the distinct entries of $\boldsymbol{M}$.

III. Classification Architecture Design

The classification architecture devised in this paper is grounded on a heuristic design criterion leading to the cascade of two binary hypothesis tests as illustrated in Fig. 1, where $\mathcal{H}_1=\{H_0,H_1\}$. In Fig. 1, the first stage rejects H_2 by understanding the homogeneity of the secondary data and, if

[1] Actually, the considered partially-homogeneous environment is slightly different from the classical one since we also consider the presence of thermal noise.

homogeneous, we discriminate between H_0 and H_1. At each stage, the GLRT design criterion is exploited as shown below.

The first stage is aimed at discriminating between $\mathcal{H}_1$ and H_2. To this end, we exploit the following GLRT

$$\frac{\max\limits_{\boldsymbol{\theta}_2} f_{S_2}(\boldsymbol{Z}_S;\boldsymbol{\theta}_2)}{\max\limits_{\boldsymbol{\theta}_0} f_{S_0}(\boldsymbol{Z}_S;\boldsymbol{\theta}_0)} \underset{\mathcal{H}_1}{\overset{H_2}{\gtrless}} \eta_1, \tag{3}$$

where η_1 is the threshold set to guarantee the pre-assigned misclassification probability. Following the lead of [14] and [21], the compressed log-likelihood of $\boldsymbol{Z}_S$ under H_0 can be written as

$$\begin{aligned} h_0'(\boldsymbol{Z}_S;\widehat{\boldsymbol{\theta}}_0') &= -K_S\left[\sum_{i=1}^{r}\log\frac{\mu_{S,i}}{K_S}+(N-r)\log\widehat{\sigma}_{(0)}^2\right] \\ &\quad -K_S N\log\pi - K_S N, \end{aligned} \tag{4}$$

where $\widehat{\boldsymbol{\theta}}_0'$ is the estimate of $\boldsymbol{\theta}_0$, $\widehat{\sigma}_{(0)}^2=\frac{1}{K_S(N-r)}\sum_{i=r+1}^{N}\mu_{S,i}$ with $\mu_{S,1}\geq\ldots\geq\mu_{S,N}\geq 0$ the eigenvalues of $\boldsymbol{Z}_S\boldsymbol{Z}_S^\dagger$.

On the other hand, in order to maximize $f_{S_2}(\boldsymbol{Z}_S;\boldsymbol{\theta}_2)$ over $\boldsymbol{\theta}_2$, exploiting *Theorem 1* in [22] we obtain

$$\begin{aligned} &-\mathrm{Tr}\left[\left(\sigma^2\boldsymbol{I}+\boldsymbol{\Lambda}\right)^{-1}\boldsymbol{U}^\dagger\boldsymbol{V}_1\boldsymbol{\Theta}_1\boldsymbol{V}_1^\dagger\boldsymbol{U}\right] \\ &\qquad -\mathrm{Tr}\left[\left(\sigma^2\boldsymbol{I}+\boldsymbol{\Gamma}_2\boldsymbol{\Lambda}\boldsymbol{\Gamma}_2\right)^{-1}\boldsymbol{U}^\dagger\boldsymbol{V}_2\boldsymbol{\Theta}_2\boldsymbol{V}_2^\dagger\boldsymbol{U}\right] \\ &\leq -\mathrm{Tr}\left[\left(\sigma^2\boldsymbol{I}+\boldsymbol{\Lambda}\right)^{-1}\boldsymbol{\Theta}_1\right]-\mathrm{Tr}\left[\left(\sigma^2\boldsymbol{I}+\boldsymbol{\Gamma}_2\boldsymbol{\Lambda}\boldsymbol{\Gamma}_2\right)^{-1}\boldsymbol{\Theta}_2\right], \end{aligned} \tag{5}$$

where $\boldsymbol{\Theta}_1$ and $\boldsymbol{\Theta}_2$ are diagonal matrices containing the eigenvalues of $\boldsymbol{Z}_{S_1}\boldsymbol{Z}_{S_1}^\dagger$ and $\boldsymbol{Z}_{S_2}\boldsymbol{Z}_{S_2}^\dagger$, respectively, with $\boldsymbol{Z}_{S_1}=[\boldsymbol{r}_1,\ldots,\boldsymbol{r}_{K_1}]$ and $\boldsymbol{Z}_{S_2}=[\boldsymbol{r}_{K_1+1},\ldots,\boldsymbol{r}_{K_S}]$. $\boldsymbol{V}_1\in\mathbb{C}^{N\times N}$ and $\boldsymbol{V}_2\in\mathbb{C}^{N\times N}$ are the unitary matrix of corresponding eigenvectors of $\boldsymbol{\Theta}_1$ and $\boldsymbol{\Theta}_2$, respectively. Then it is easy to show that the maximization with respect to $\boldsymbol{\theta}_2$ consequently leads to the following compressed log-likelihood function

$$\begin{aligned} h_2'(\boldsymbol{Z}_S;\widehat{\boldsymbol{\theta}}_2') = \max_{\substack{K_1=r,\\ \ldots,K_S-r}} \Bigg\{ &-K_S N\log\pi - K_1\sum_{i=1}^{r}\log\frac{\mu_{1,i}}{K_1} \\ &-K_C\sum_{i=1}^{r}\log\frac{\mu_{2,i}}{K_C}-K_S(N-r)\log\widehat{\sigma}_{(2)}^2-K_S N\Bigg\}, \end{aligned} \tag{6}$$

where $\widehat{\sigma}_{(2)}^2=\frac{1}{K_S(N-r)}\sum_{i=r+1}^{N}(\mu_{1,i}+\mu_{2,i})$.

Thus, the GLRT in (3) can be written as

$$h_2'(\boldsymbol{Z}_S;\widehat{\boldsymbol{\theta}}_2')-h_0'(\boldsymbol{Z}_S;\widehat{\boldsymbol{\theta}}_0')\underset{\mathcal{H}_1}{\overset{H_2}{\gtrless}}\eta_1. \tag{7}$$

If $\mathcal{H}_1$ is declared, in the second stage we decide whether the secondary data have the same clutter covariance with primary data through the following GLRT

$$\frac{\max\limits_{\boldsymbol{\theta}_1} f_1(\boldsymbol{Z};\boldsymbol{\theta}_1)}{\max\limits_{\boldsymbol{\theta}_0} f_0(\boldsymbol{Z};\boldsymbol{\theta}_0)}\underset{H_0}{\overset{H_1}{\gtrless}}\eta_2, \tag{8}$$

where η_2 is the threshold. The maximization problem under H_1 can be written as

$$\begin{aligned} &\max_{\sigma^2,\boldsymbol{\Lambda},\boldsymbol{U},\boldsymbol{\Gamma}_1} -K_S\log\det\left(\sigma^2\boldsymbol{I}+\boldsymbol{\Gamma}_1\boldsymbol{\Lambda}\boldsymbol{\Gamma}_1\right) \\ &-K_P\log\det\left(\sigma^2\boldsymbol{I}+\boldsymbol{\Lambda}\right)-\sum_{k=1}^{K_P}\boldsymbol{z}_k^\dagger\boldsymbol{U}(\sigma^2\boldsymbol{I}+\boldsymbol{\Lambda})^{-1}\boldsymbol{U}^\dagger\boldsymbol{z}_k \\ &-\sum_{k=1}^{K_S}\boldsymbol{r}_k^\dagger\boldsymbol{U}(\sigma^2\boldsymbol{I}+\boldsymbol{\Gamma}_1\boldsymbol{\Lambda}\boldsymbol{\Gamma}_1)^{-1}\boldsymbol{U}^\dagger\boldsymbol{r}_k. \end{aligned} \tag{9}$$

In this stage, we show that a suboptimum estimate of $\boldsymbol{U}$, denoted by $\widehat{\boldsymbol{U}}$, can be obtained by minimizing a specific residual error between data centroid and the direction of minimum energy. The proof is omitted for brevity. Meanwhile, we estimate λ_i following the lead of [14] with primary data only. Specifically, $\widehat{\sigma}^2=\frac{1}{K_P(N-r)}\sum_{i=r+1}^{N}\mu_i$, and $\widehat{\lambda}_i=\max\left\{\frac{1}{K_P}\mu_i-\widehat{\sigma}^2,0\right\}$, $i=1,\ldots,r$, where $\mu_1\geq\ldots\geq\mu_N\geq 0$ are the eigenvalues of $\boldsymbol{Z}_P\boldsymbol{Z}_P^\dagger$. As for $\gamma_{i,1}$, $i=1,\ldots,r$, under the constraint that $\gamma_{1,1}\geq\ldots\geq\gamma_{r,1}>0$, we introduce $\gamma_{i,1}=\sum_{j=i}^{r}\tau_{j,p}$, $i=1,\ldots,r$, where $\tau_{r,p}>0$, and $\tau_{i,p}\geq 0$, $i=1,\ldots,r-1$. Thus the estimates of $\widehat{\gamma}_{i,1}$, $i=1,\ldots,r$, are given by $\widehat{\gamma}_{i,1}=\sum_{j=i}^{r}\widehat{\tau}_{j,p}$, $i=1,\ldots,r$. The compressed log-likelihood of $\boldsymbol{Z}$ under H_1 can thus be written as

$$\begin{aligned} h_1(\boldsymbol{Z};\widehat{\boldsymbol{\theta}}_1) = &-(K_P+K_S)(N-r)\log\widehat{\sigma}^2-\sum_{i=1}^{r}\frac{\boldsymbol{S}_P(i,i)}{\widehat{\sigma}^2+\widehat{\lambda}_i} \\ &-\sum_{i=r+1}^{N}\frac{\boldsymbol{S}_P(i,i)}{\widehat{\sigma}^2}-\sum_{i=1}^{r}\frac{\boldsymbol{S}_S(i,i)}{\widehat{\sigma}^2+\widehat{\gamma}_{i,1}\widehat{\lambda}_i}-\sum_{i=r+1}^{N}\frac{\boldsymbol{S}_S(i,i)}{\widehat{\sigma}^2} \\ &-K_P\sum_{i=1}^{r}\log\left(\widehat{\sigma}^2+\widehat{\lambda}_i\right)-K_S\sum_{i=1}^{r}\log\left(\widehat{\sigma}^2+\widehat{\gamma}_{i,1}\widehat{\lambda}_i\right), \end{aligned} \tag{10}$$

with $\boldsymbol{S}_P=\sum_{k=1}^{K_P}\widehat{\boldsymbol{U}}^\dagger\boldsymbol{z}_k\boldsymbol{z}_k^\dagger\widehat{\boldsymbol{U}}$ and $\boldsymbol{S}_S=\sum_{k=1}^{K_S}\widehat{\boldsymbol{U}}^\dagger\boldsymbol{r}_k\boldsymbol{r}_k^\dagger\widehat{\boldsymbol{U}}$.

Then, under H_0, even though it is possible to obtain the exact MLEs as shown in (4), we approximate the compressed likelihood as under H_1 so that vectors undergo the same approximated transformation represented by $\boldsymbol{U}$. It is easy to show that the compressed log-likelihood function under H_0 is

$$\begin{aligned} h_0(\boldsymbol{Z};\widehat{\boldsymbol{\theta}}_0) = &-\sum_{i=1}^{r}\frac{\boldsymbol{S}_Z(i,i)}{\widehat{\sigma}^2+\widehat{\lambda}_i}-\sum_{i=r+1}^{N}\frac{\boldsymbol{S}_Z(i,i)}{\widehat{\sigma}^2} \\ &-(K_P+K_S)\left[\sum_{i=1}^{r}\log\left(\widehat{\sigma}^2+\widehat{\lambda}_i\right)+(N-r)\log\widehat{\sigma}^2\right], \end{aligned} \tag{11}$$

with $\boldsymbol{S}_Z=\widehat{\boldsymbol{U}}^\dagger\boldsymbol{Z}\boldsymbol{Z}^\dagger\widehat{\boldsymbol{U}}$. The logarithm of the GLRT in the second stage can be written as

$$h_1(\boldsymbol{Z};\widehat{\boldsymbol{\theta}}_1)-h_0(\boldsymbol{Z};\widehat{\boldsymbol{\theta}}_0)\underset{H_0}{\overset{H_1}{\gtrless}}\eta_2. \tag{12}$$

In the case that r is unknown, we have to estimate it from data. To this end, we devise a preliminary stage that provides

the estimate of r by means of the Model Order Selection (MOS) rules [23], [24]. The estimate of r exploiting the Akaike Information Criterion (AIC), Generalized Information Criterion (GIC), Bayesian Information Criterion (BIC) is given by $r = \arg\min_{r=1,\ldots,M} \left\{ -2h_0'(\boldsymbol{Z}_S; \widehat{\boldsymbol{\theta}}_0') + \kappa \cdot p(r) \right\}$, where $M < N$ is an upper bound on r, $h_0'(\boldsymbol{Z}_S; \widehat{\boldsymbol{\theta}}_0')$ is given by (4), and $\kappa \cdot p(r)$ is the penalty term with $p(r) = r(2N - r) + 1$ the number of unknown parameters [25] and

$$\kappa = \begin{cases} 2, & \text{AIC}, \\ (1+\rho), \ \rho \geq 1 & \text{GIC}, \\ \log(2NK_S), & \text{BIC}. \end{cases} \tag{13}$$

IV. Illustrative Examples

In this section, we investigate the classification performance of the proposed architectures in terms of the Probability of Correct Classification (P_{cc}), by means of standard Monte Carlo counting techniques. Specifically, we compute P_{cc} and the Root Mean Square (RMS) estimation errors of clutter edge positions over $M = 1000$ independent trials. The numerical examples assume that $N = 9$, $K_P = 8$, $K_S = 32$, $K_1 = 20$, and $\sigma^2 = 1$. The clutter covariance matrix of primary data is defined as $\boldsymbol{M} = \sigma_c^2 \sum_{\theta_i \in \Theta} \boldsymbol{v}(\theta_i)\boldsymbol{v}(\theta_i)^\dagger$, where σ_c^2 is the clutter power set according to the Clutter to Noise Ratio (CNR) defined as CNR $= 10\log(\sigma_c^2/\sigma^2) = 30$ dB, $\Theta = \{-20°, 0°, 10°\}$ implying that the true rank of the clutter covariance matrix is $r = 3$, and the steering vector is given by $\boldsymbol{v}(\theta_i) = \frac{1}{\sqrt{N}} \left[1, e^{\jmath\pi \sin\theta_i}, \ldots, e^{\jmath\pi(N-1)\sin\theta_i}\right]$. As for γs, we assume that $\omega_{(1),l} \geq \ldots \geq \omega_{(r),l}$, $l = 1, 2$, are ordered uniformly distributed random variables, and $\gamma_{i,l} = \Delta_l \omega_{(i),l}$, $i = 1, \ldots, r$, $l = 1, 2$, where Δ_l, $l = 1, 2$, are determined according to the Clutter Power Ratio (CPR) under H_l, $l = 1, 2$, given by $\text{CPR}_l = 10\log\Delta_l$, $l = 1, 2$. Moreover, we evaluate the thresholds under each stage according to a false classification probability $P_{FC} = 0.05$ by means of Monte Carlo techniques resorting to $100/P_{FC}$ independent trials.

First of all, we focus on the performance of rank estimation. In Fig. 2, we show the percentage of estimation of the BIC rule under each hypothesis with different parameters (results not shown here indicate that the BIC rule returns better performance than AIC and GIC). As can be observed, the preliminary stage returns a correct estimation probability no less than 0.997 for all the considered situations. In this respect, in the following classification performance analysis we assume that the true value of r is known.

Table I contains the classification results of 1000 trials when data are generated under H_0. Inspection of the Table highlights that the classification procedure correctly decides for H_0 with a P_{cc} greater than 0.95.

In Fig. 3 we proceed with the performance under H_l, $l = 1, 2$, and plot the P_{cc} under each hypothesis versus CPR_l. Specifically, Fig. 3(a) shows that under H_1, the system ensures $P_{cc} \geq 0.9$ when $\text{CPR}_1 \geq 20$ dB. Meanwhile, when CPR_1 is too small, H_1 cannot be correctly classified since the power variation between the primary and secondary data is too low to be identified. Fig. 3(b) deals with the case when H_2 is true and

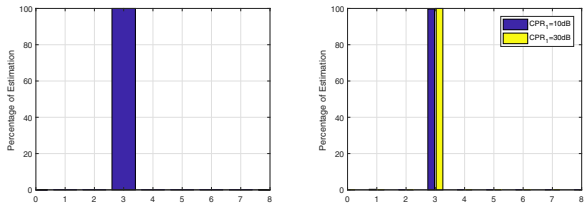

(a) H_0 (b) H_1

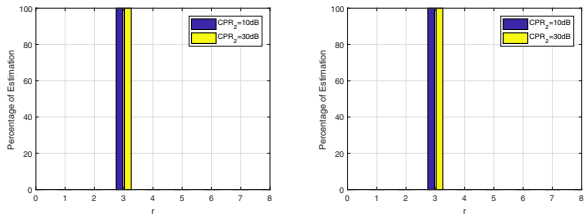

(c) H_2, $K_1 = 4$ (d) H_2, $K_1 = 10$

Fig. 2: Rank estimation performance under each hypothesis

the curve highlights that the clutter edge in the secondary data characterized by $\text{CPR}_2 \geq 20$ dB can be correctly classified since the power transitions become nonnegligible.

TABLE I: Classification results under H_0

H_0	H_1	H_2
951	0	49

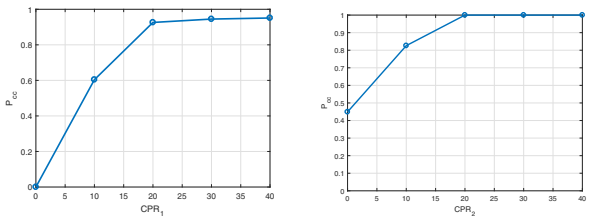

(a) P_{cc} versus CPR_1 under H_1 (b) P_{cc} versus CPR_2 under H_2

Fig. 3: Classification performance under each hypothesis

The final analysis focuses on the estimation capabilities of the proposed approach for what concerns the position of the clutter edge. In addition, the edge index K_1 is generated as discrete uniform random variables taking on values in $K_1 \in \{r, \ldots, K_S - r\}$. Fig. 4 depicts the RMS estimation error against CPR_2 and highlights that when $\text{CPR}_2 \geq 30$ dB, the estimation with respect to K_1 can ensure an error with RMS < 1 and achieve accurate estimates when $\text{CPR}_2 \geq 40$ dB.

V. Conclusion

In this paper, we focused on the radar operating scenario classification problem and devised a heuristic architecture

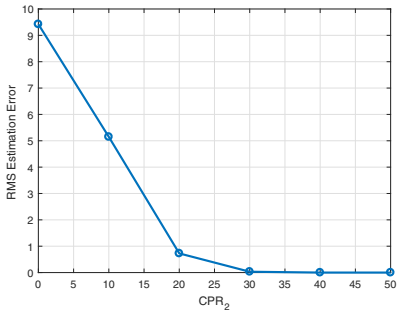

Fig. 4: RMS versus CPR_2 under H_2

which is the cascade of two stages solving two binary hypothesis test, respectively. Such an information is crucial for the the selection of the most appropriate decision scheme for target detection tasks. In this context, the GLRT-based approach was applied at each stage and the simulation results highlighted the effectiveness of the proposed architecture. Future research tracks may include the classification architecture design in the presence of more challenging scenarios, accounting for more clutter edges or fully-heterogeneous environment.

REFERENCES

[1] E. J. Kelly, "An adaptive detection algorithm," *IEEE Transactions on Aerospace and Electronic Systems*, vol. 22, no. 1, pp. 115–127, 1986.

[2] F. C. Robey, D. R. Fuhrmann, R. Nitzberg, and E. J. Kelly, "CFAR adaptive matched filter detector," *IEEE Transactions on Aerospace and Electronic Systems*, vol. 28, no. 1, pp. 208–216, 1992.

[3] C. Hao, D. Orlando, G. Foglia, and G. Giunta, "Knowledge-based adaptive detection: Joint exploitation of clutter and system symmetry properties," *IEEE Signal Processing Letters*, vol. 23, no. 10, pp. 1489–1493, 2016.

[4] C. Hao, S. Gazor, G. Foglia, B. Liu, and C. Hou, "Persymmetric adaptive detection and range estimation of a small target," *IEEE Transactions on Aerospace and Electronic Systems*, vol. 51, no. 4, pp. 2590–2604, October 2015.

[5] D. Orlando and G. Ricci, "Adaptive radar detection and localization of a point-like target," *IEEE Transactions on Signal Processing*, vol. 59, no. 9, pp. 4086–4096, 2011.

[6] D. Orlando and G. Ricci, "A Rao test with enhanced selectivity properties in homogeneous scenarios," *IEEE Transactions on Signal Processing*, vol. 58, no. 10, pp. 5385–5390, October 2010.

[7] C. Hao, D. Orlando, G. Foglia, X. Ma, S. Yan, and C. Hou., "Persymmetric adaptive detection of distributed targets in partially-homogeneous environment," *Digital signal processing*, vol. 24, no. 1, pp. 42–51, 2014.

[8] G. Foglia, C. Hao, A. Farina, D. Orlando, and C. Hou, "Adaptive detection of point-like targets in partially homogeneous clutter with symmetric spectrum," *IEEE Transactions on Aerospace and Electronic Systems*, vol. 53, no. 4, pp. 2110–2119, August 2017.

[9] C. Hao, D. Orlando, X. Ma, and C. Hou, "Persymmetric Rao and Wald tests for partially homogeneous environment," *IEEE Signal Processing Letters*, vol. 19, no. 9, pp. 587–590, September 2012.

[10] L. Yan, C. Hao, D. Orlando, A. Farina, and C. Hou, "Parametric space-time detection and range estimation of point-like targets in partially homogeneous environment," *IEEE Transactions on Aerospace and Electronic Systems*, vol. 56, no. 2, pp. 1228–1242, 2020.

[11] C. Hao, D. Orlando, A. Farina, S. Iommelli, and C. Hou, "Symmetric spectrum detection in the presence of partially homogeneous environment," in *IEEE Radar Conference (RadarConf)*, May 2016, pp. 1–4.

[12] C. Hao, D. Orlando, G. Foglia, X. Ma, and C. Hou, "Adaptive radar detection and range estimation with oversampled data for partially homogeneous environment," *IEEE Signal Processing Letters*, vol. 52, no. 2, pp. 603–616, 2016.

[13] A. D. Maio, C. Hao, and D. Orlando, "An adaptive detector with range estimation capabilities for partially homogeneous environment," *IEEE Signal Processing Letters*, vol. 21, no. 3, pp. 325–329, May 2014.

[14] D. Xu, P. Addabbo, C. Hao, J. Liu, D. Orlando, and A. Farina, "Adaptive strategies for clutter edge detection in radar," *Signal Processing*, vol. 186, p. 108127, 2021. [Online]. Available: https://www.sciencedirect.com/science/article/pii/S0165168421001651

[15] V. Carotenuto, A. D. Maio, D. Orlando, and P. Stoica, "Radar detection architecture based on interference covariance structure classification," *IEEE Transactions on Aerospace and Electronic Systems*, vol. 55, no. 2, pp. 607–618, April 2019.

[16] M. E. Smith and P. K. Varshney, "Intelligent CFAR processor based on Data Variability," *IEEE Transactions on Aerospace and Electronic Systems*, vol. 36, no. 3, pp. 837–847, July 2000.

[17] P. Addabbo, S. Han, D. Orlando, and G. Ricci, "Learning strategies for radar clutter classification," *IEEE Transactions on Signal Processing*, vol. 69, pp. 1070–1082, 2021.

[18] A. P. Dempster, N. M. Laird, and D. B. Rubin, "Maximum likelihood from incomplete data via the EM algorithm," *J. Rou. Stat. Soc. (Series B.-Methodological)*, vol. 39, no. 1, pp. 1–38, 1977.

[19] E. Conte, A. De Maio, and G. Ricci, "GLRT-based adaptive detection algorithms for range-spread targets," *IEEE Transactions on Signal Processing*, vol. 49, no. 7, pp. 1336–1348, July 2001.

[20] M. A. Richards, W. L. Melvin, J. A. Scheer, and W. A. Holm, *Principles of Modern Radar: Radar Applications, Volume 3*, ser. Electromagnetics and Radar. Institution of Engineering and Technology, 2013.

[21] L. Yan, P. Addabbo, C. Hao, D. Orlando, and A. Farina, "New EC-CM techniques against Noise-like and /or Coherent Interferers," *IEEE Transactions on Aerospace and Electronic Systems*, vol. 56, no. 2, pp. 1172–1188, 2019.

[22] L. Mirsky, "On the trace of matrix products," *Mathematische Nachrichten*, vol. 20, no. 3-6, pp. 171–174, 1959.

[23] P. Stoica and Y. Selen, "Model-order selection: A review of information criterion rules," *IEEE Signal Processing Magazine*, vol. 21, no. 4, pp. 36–47, 2004.

[24] P. Stoica, Y. Selen, and J. Li, "On information criteria and the generalized likelihood ratio test of model order selection," *IEEE Signal Processing Letters*, vol. 11, no. 10, pp. 794–797, 2004.

[25] H. L. V. Trees, *Optimum Array Processing (Detection, Estimation, and Modulation Theory, Part IV)*, John Wiley & Sons, 2004.